

Ultrafast Investigation of Vibrational Relaxation and Solvent Coordination Following Photodissociation of $\text{Cr}(\text{CO})_6$

Seuk-Beum Ko*, Soo-Chang Yu*, and J. B. Hopkins

*Department of Chemistry Education, Chonbuk National University, Chonju, Chonbuk 560-756, Korea

*Department of Chemistry, Kunsan National University, Kunsan, Chonbuk 573-360, Korea

Department of Chemistry, Louisiana State University, Baton Rouge, LA 70803, U. S. A.

Received May 7, 1994

Picosecond time-resolved resonance Raman spectroscopy has been used to study the photochemistry of $\text{Cr}(\text{CO})_6$ in cyclohexane following photoexcitation at 266 nm. Photodissociative loss of CO is found to occur within our pulse width of ≤ 5 ps by probing the 533 cm^{-1} vibrational mode of ground state $\text{Cr}(\text{CO})_6$. The subsequent dynamics after photodissociation are interpreted in terms of solvation, vibrational and electronic relaxations. The vibrational relaxation time of 100 ps and 83 ps are observed by monitoring $\nu=0$ and $\nu=1$ of the 381 cm^{-1} transient mode, respectively. No evidence was found for solvation and electronic relaxation occurring on a time scale of ≥ 5 ps.

Introduction

The photochemistry of $\text{Cr}(\text{CO})_6$ has been extensively investigated¹. Recent studies have focused on the time scale of the photodissociation and the subsequent dynamics of the photogenerated $\text{Cr}(\text{CO})_5$ fragment in solution.²⁻⁹ The dynamics of photoproduct $\text{Cr}(\text{CO})_5$ are of interest as a probe of condensed phase processes such as solvent coordination, solvent reorientation, electronic and vibrational relaxation.^{3,6,8}

There are currently several controversies for the time scales and mechanisms of the solvent coordinated $\text{Cr}(\text{CO})_5$ photoproduct formation.²⁻⁹ Time-resolved picosecond absorption studies by Simon *et al.*²⁻³ first showed that the photodissociation of $\text{Cr}(\text{CO})_6$ results in the formation of solvated $\text{Cr}(\text{CO})_5$, which appears in a time scale of ≤ 0.8 ps in cyclohexane. In their model, solvent coordination takes place after dissipation of the excess energy by electronic relaxation.

However, in contrast to these results the picosecond transient infrared experiments by Spears *et al.*⁵ suggested a much longer solvent coordination time of 200 ps. Femtosecond transient absorption experiments by Nelson *et al.*⁴ showed two different time scales of 300 fs and 70 ps in methanol. The short 300 fs time scale was interpreted as photodissociation immediately followed by solvation. The long 70 ps time scale was assigned to both electronic and vibrational relaxation from the excited state of the $\text{Cr}(\text{CO})_5\text{-S}(\text{S}; \text{solvent})$ complex. Further transient absorption studies by Harris *et al.*⁷⁻⁸ reported a time scale of 4 to 17 ps which has been interpreted as vibrational relaxation in the pentacarbonyl photoproduct.

To provide further insight into this photochemistry, we have used transient picosecond Raman spectroscopy to directly probe the vibrational spectrum of the photoproduct. In the previous report⁹ vibrational relaxation has been suggested to occur on a time scale of 100 ps. But, this conclusion was made with the assistance of complementary Stokes and anti-Stokes intensity changes by recording them only at 3 different times with a pulse width of ≥ 30 ps.

Here we are to determine the identity of the photogenerated transients and investigate the time scale of photodissociation, solvation and vibrational relaxation by utilizing the feature of the transient Raman spectroscopy, which monitors dire-

ctly the vibrational modes of interest. An elaborate transient Raman investigation is carried out by using a ≤ 5 ps pulse width at 266 nm, and the dynamics are taken precisely with a 5 ps step size while probing the relevant vibrational modes.

Experimental

The experimental apparatus has been described in detail elsewhere¹⁰⁻¹¹. The laser system consists of a high repetition rate (2 kHz) chirped pulse regenerative amplifier which provides 1 mJ pulses with an 8ps pulse width at $1.064\text{ }\mu\text{m}$. The 266 nm frequency quadrupled pulse has a width of ≤ 5 ps. Laser excitation occurs in a free flowing jet which moves the solution at a speed sufficient to ensure that no two successive pulses interrogate the same region of sample. Raman scattering is dispersed by an instruments SA U1000 double monochromator. The signal is detected by a photomultiplier tube, and processed by a gated integrator. The accuracy of the monochromator is specified at $\pm 1\text{ cm}^{-1}$ over 5000 cm^{-1} . $\text{Cr}(\text{CO})_6$ is photodissociated at 266 nm and the transient is probed at the same wavelength with a second laser pulse. The pure transient Raman spectrum is obtained by using a two-pulse spectrum differencing technique. This is accomplished by rapidly chopping (mechanically) the pump and the probe beams, and recording the total two pulse spectrum as well as the individual one-pulse background spectrum. Dynamics are obtained by varying the optical delay between the pump and the probe pulses using a retroreflector and a 1 m long computer controlled delay stage. The timing between two pulses was measured experimentally using the dynamics of the anti-Stokes spectrum of the supposed $\text{Cr}(\text{CO})_5\text{-S}(\text{S}; \text{solvent})$. The time axis in the spectrum corresponds to the optical delay with respect to perfect temporal overlap at time zero. As a result, the time "minus" data corresponds to one of the pulses acting as the probe and the time "plus" data to the other pulse acting as the probe.

$\text{Cr}(\text{CO})_6$ (99% purity) was purchased from Aldrich and used without further purification. The concentration was 10 mM in every solvent. Cyclohexane was purchased from Aldrich and was of spectrograde purity. Tetrahydrofuran (THF), methanol, and *n*-propanol were HPLC purity and were purchased from Mallinckrodt.

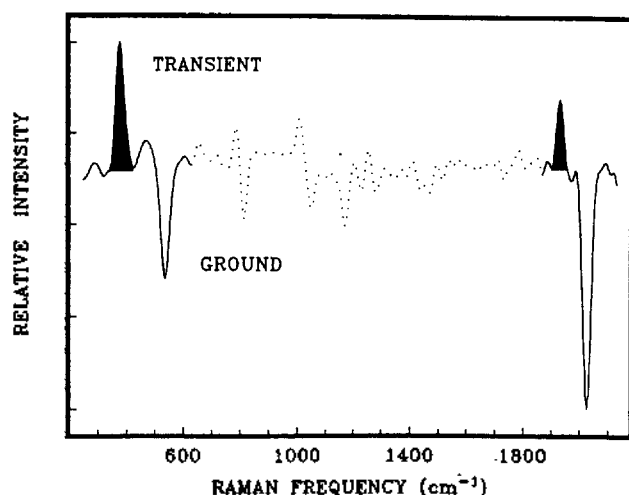


Figure 1. Long range transient difference spectrum of $\text{Cr}(\text{CO})_5\text{-S}$ in cyclohexane. Time delay between pulses is 400 ps. The filled-in peaks corresponds to the transient bands. Negative going peaks are ground state $\text{Cr}(\text{CO})_5$ bands. The dotted region of the spectrum has a low signal-to-noise due to the subtraction of intense cyclohexane solvent bands.

Results and Discussion

Figure 1 shows the transient Raman spectrum for $\text{Cr}(\text{CO})_5$ in cyclohexane obtained by using a two-pulse spectrum differencing technique. This is achieved mathematically by computing the transient spectrum as: Transient Spectrum = Two-Pulse Spectrum - One-Pulse Spectrum \times factor. The factor is adjusted such that the solvent bands subtract to zero in the computed transient Raman spectrum. Two-Pulse spectrum contains the transient and ground state spectrum because as soon as the pump beam generates transients the following probe beam probes the transients as well as the ground state molecules. On the other hand, one-pulse spectrum contains only ground state spectrum because the probe beam probes only the ground state molecules in the absence of the pump beam. It is for this reason that the two-pulse spectrum differencing technique is used. This spectrum is believed to be the pure transient Raman spectrum.

There are two kinds of bands in terms of direction in this transient Raman spectrum. One is for the negative-going bands at 533 cm^{-1} and 2091 cm^{-1} , and the other is for the positive-going bands (filled-in) at 381 cm^{-1} and 1935 cm^{-1} . Compared to the normal ground state Raman spectrum¹² of gas phase $\text{Cr}(\text{CO})_5$ which has a ν_3 CO stretch at 2019 cm^{-1} and the ν_2 Cr-CO stretch vibration at 381 cm^{-1} , the transient bands at 1935 cm^{-1} and 381 cm^{-1} are likely to be CO stretching and Cr-CO stretching vibrations, respectively. The Raman band of $\text{Cr}(\text{CO})_5$ at 381 cm^{-1} does not appear to bleach because of the large positive transient band at or near the same frequency.

The negative-going bands are caused by changes in the optical density of the solution due to the transient absorption of the photoproducts and the photobleaching of ground state $\text{Cr}(\text{CO})_5$. But this change in the optical density does not have an effect on vibrational frequency or Raman shift of the band in ground state. Raman shifts of the negative bands therefore appear in the same places as those of ground state $\text{Cr}(\text{CO})_5$.

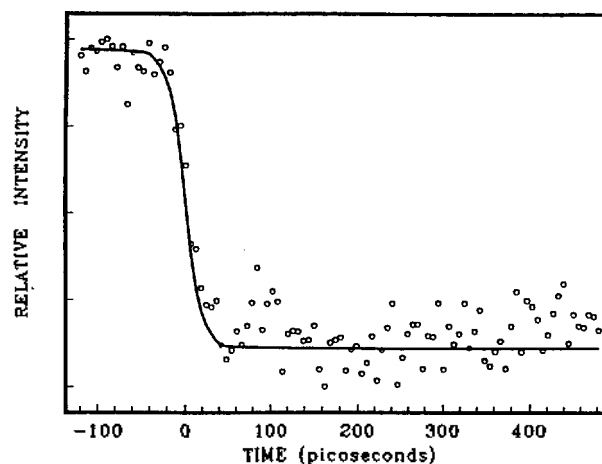


Figure 2. Dynamics for the intensity change of the negative-going peak at 533 cm^{-1} . Positive times correspond to pump followed by delayed probe. Relative energies are approximately 15 μJ for the pump and 3 μJ for the probe. Step size of the optical delay is 5 ps. The solid line through the data represents a 5 ps decay time.

The monitoring of negative bands thus provides information on the phenomena occurring in ground state $\text{Cr}(\text{CO})_5$. The dynamics of the negative bands, for instance, accounts for the population change with time in ground state $\text{Cr}(\text{CO})_5$ resulting from photodissociation. This is illustrated in Figure 2 of which dynamics is obtained from the negative-going band at 533 cm^{-1} in the Stokes side. The Raman signal has a maximum value in intensity in the region of negative time and has a minimum value in the region of positive time while showing an inflection point at time zero. In the region of negative time where the probe beam comes earlier than the pump beam to the sample, most of $\text{Cr}(\text{CO})_5$ molecules are in their ground state. As a result the intensity of the Raman signal proportional to the number of ground state molecules maintains a maximum value. On the contrary, in the region of positive time where the pump beam comes earlier than the probe beam, the ground state molecules are bleached due to photodissociation. And so, the intensity of the Raman signal falls off to a minimum value. This dynamics is fitted to take place within our pulse width. This fact provides strong evidence that photodissociation occurs within 5 ps. The photodissociation of $\text{Cr}(\text{CO})_5$ leads to the photoproduct $\text{Cr}(\text{CO})_5^{13}$ and in turn, solvation finally.

The filled-in positive bands appeared in Figure 1 seems more likely to be those of solvated $\text{Cr}(\text{CO})_5$ than those of naked one for the following three major reasons. First, the lifetime of the transient is found to be longer than 1 ns (not shown) and is consistent with the known millisecond lifetime¹⁴ for solvated $\text{Cr}(\text{CO})_5$. Moreover, the lifetime of longer than 200 ps for a naked $\text{Cr}(\text{CO})_5$ has not been suggested by any group yet. Secondly, the laser power used in this experiment is 10 to 25 times weaker than that used in the previous transient infrared⁵ or transient UV-visible absorption^{2-4,7} studies where only $\text{Cr}(\text{CO})_5\text{-S}$ was identified as a photoproduct. Thirdly, the linearity of the transient signal was checked over a range of laser powers from 5 times greater to 5 times less than those typically used. Only at the highest laser power was a nonlinear signal observed. In fact, the transient

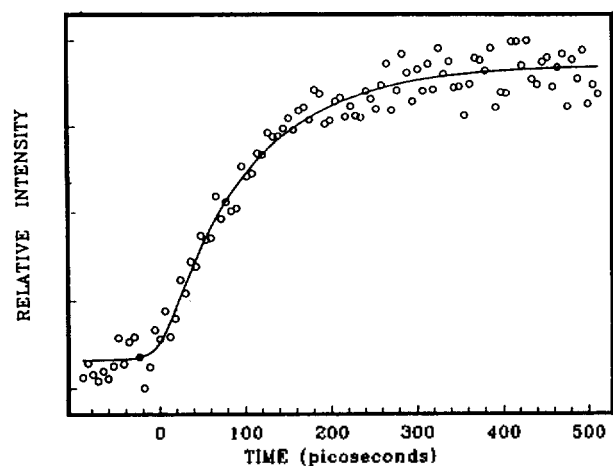


Figure 3. Dynamics for the intensity change of the Stokes band at 381 cm^{-1} . The rise time obtained from the single exponential curve fitting is 100 ps.

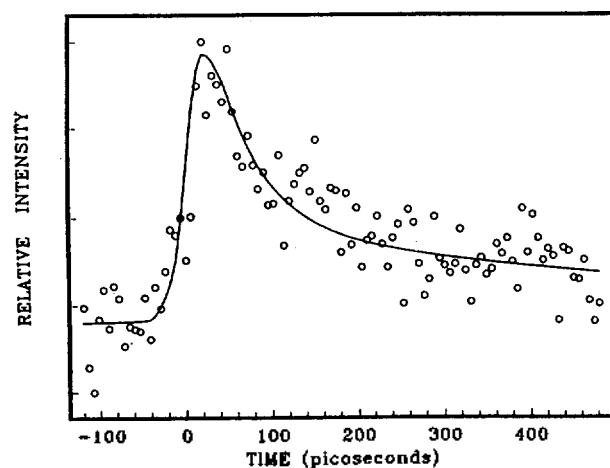


Figure 4. Dynamics for the intensity change of the anti-Stokes band at 381 cm^{-1} . The decay time obtained from the single exponential curve fitting is 83 ps.

signal was found to decrease at high power. The observation of a transient signal linear in both pump and probe laser power is a good indication that the transient is $\text{Cr}(\text{CO})_5\text{-S}$ and not $\text{Cr}(\text{CO})_n$, where $n \leq 4$. In this respect, the filled-in positive bands are considered to be those of the transient $\text{Cr}(\text{CO})_5\text{-S}$. A naked $\text{Cr}(\text{CO})_5$ might be formed within our pulse width of 5 ps and immediately followed by solvation, supporting the transient absorption studies.

The dynamics for the transient has a 100 ps rise time as shown in Figure 3 with a single exponential, which suggests that a single step of photochemistry is involved. This dynamics were monitored at 381 cm^{-1} in the Stokes region. The anti-Stokes dynamics monitored at 381 cm^{-1} also show a single exponential with 83 ps decay time as shown in Figure 4. The difference in time scale between the growing Stokes and the decaying anti-Stokes dynamics is somewhat unusual. In principle, the intensity of Stokes scattering is mainly responsible for the number of molecules in $v=0$ (the lowest vibrational quantum number) and its dynamics reflect the population change of the molecules in $v=0$ with time;

the more the molecules, the bigger the intensity. In a similar fashion, the intensity of anti-Stokes scattering is responsible for the number of molecules in $v=1$ and its dynamics reflect the population change of the molecules in $v=1$. As a consequence, if vibrational relaxation occurs only from $v=1$ to $v=0$ of the 381 cm^{-1} mode, the time scales for both Stokes and anti-Stokes dynamics should be exactly same because the rate of population of the molecules in $v=0$ will be the same as that of depopulation in $v=1$. Therefore, it is assumed that there are some vibrational modes between $v=0$ and $v=1$ of the 381 cm^{-1} vibrational mode through complicated couplings. In such a case the energy flow from the upper vibrational levels to the $v=0$ involves more than one channel. This seems to be the reason why the rate of two dynamics are different each other. Although there exists some discrepancy in time scale between two scattering processes, the complementary observation of the growing Stokes and the decaying anti-Stokes dynamics is interpreted as the vibrational energy relaxation because the complementary dynamics of the intensity of the Stokes and anti-Stokes spectra are only consistent with vibrational energy relaxation.

The possibility of being electronic relaxation is ruled out because the Stokes and the anti-Stokes dynamics are different each other. If electronic relaxation is involved, both the Stokes and the anti-Stokes dynamics should have the same pattern with a growing intensity because the energy flow from the upper electronic energy level will populate at the same time the $v=0$ and $v=1$ in the lower electronic energy level. Instead, we observe the decay of the anti-Stokes scattering and the rise of the Stokes scattering. These dynamics are assigned to vibrational relaxation. These considerations indicate that the lower limit for the electronic relaxation time must be the time observed for the growth of the anti-Stokes band. The time constant for this process is shown to be rise time limited with an error of 5 ps (Figure 4).

It is interesting to compare the time scale for the vibrational relaxation of this molecule with the smaller as well as the bigger ones. The prototype of the small molecule which is well studied is the diatomic I_2 . The vibrational relaxation from the $v=52$ to $v=0$ of the 212 cm^{-1} mode in the electronic ground state was reported to occur on a time scale of 100 ps in our previous result¹⁵. On the contrary, the vibrational relaxation for hemoglobin which is much bigger than $\text{Cr}(\text{CO})_6$ was reported to occur within 2-5 ps¹⁶. Two kinds of mechanism for the vibrational energy relaxation are to be considered to explain the different time scales for the different molecules.

The first mechanism to be considered is an intramolecular vibrational energy relaxation. Provided that the vibrational relaxation obeys the statistical equilibrium distribution, excess energy is easily redistributed in a bigger molecule because more vibrational modes are coupled so as to dissipate excess energy efficiently. Thus the higher density of vibrational states caused by couplings of numerous vibrational modes leads to a faster relaxation¹⁷⁻¹⁸. Therefore, the extent of vibrational couplings among the vibrational modes within a molecule will have a great effect on the rate of the intramolecular vibrational energy relaxation. Considering the fact that $\text{Cr}(\text{CO})_6$ belongs to the intermediate in size among three molecules, the long time scale of 80-100 ps for the vibrational relaxation may not be easily acceptable. The plausible expla-

nation could be made by understanding the characteristics of the molecule by itself. $\text{Cr}(\text{CO})_6$ has the heavy metal, chromium, at the center of the O_h geometry, and this metal seems to be the cause of an unexpected behavior. The heavy metal might act as a blocker for the intramolecular energy transfer by preventing efficient couplings among the vibrational modes. In such a case, the vibrational energy would not be relaxed through the statistical equilibrium distribution which involves all the coupled vibrational modes. This may mainly be responsible for the long time vibrational relaxation for $\text{Cr}(\text{CO})_6$, a relatively big molecule. In the hemoglobin molecule, the iron as a heavy metal does not seem to act as much as the chromium metal as a blocker because non-metal atoms surrounding it are so numerous that the metal effect can be easily ignored.

The second mechanism is an intermolecular vibrational energy relaxation. For an intermolecular vibrational energy relaxation, either of vibrational to vibrational (V-V), vibrational to rotational (V-R), or vibrational to translational (V-T) energy transfer from the excited molecules to the surrounding solvents plays a major role. Therefore, the rate of vibrational energy relaxation mostly depends on the characteristics of the surrounding solvents. But, no solvent dependence of the vibrational energy relaxation is observed in this experiment when THF, methanol, and *n*-propanol were used to reveal the V-V, V-R or V-T energy transfer mechanisms. This means that the bond formation between the naked $\text{Cr}(\text{CO})_6$ and solvents does not affect the dynamics for 381 cm^{-1} mode corresponding to the Cr-CO stretching. If the statistical equilibrium distribution is involved in the vibrational energy relaxation before the intermolecular energy transfer, the dynamics for the vibrational energy relaxation should be contingent upon different solvents attached because different vibrational quantum states are formed due to solvents. This is another evidence that excess energy is not relaxed through the statistical equilibrium distribution.

The discrepancy in time scales for the vibrational relaxation obtained from the transient Raman and the transient absorption techniques may be resulted from the probing of different vibrational modes as well as different vibrational quantum states. Making a comparison between high and low vibrational modes, higher vibrational modes are usually subject to faster vibrational energy relaxation than are lower ones. For a given vibrational mode, higher vibrational quantum levels dissipate excess energy faster than lower ones. These facts possibly account for the big difference between the transient and the Raman results. In this respect, the 4-17 ps time scale obtained from the transient absorption method may be due to the high vibrational quantum levels of uncertain vibrational modes, whereas the 80-100 ps from the transient Raman, the low vibrational mode as well as

the low vibrational quantum levels at $v=0$ (Stokes) and $v=1$ (anti-Stokes).

Conclusion

Picosecond transient Raman spectroscopy has been used to elucidate the ultrafast phenomena upon photoexcitation. Two-pulse spectrum differencing technique was used to measure transient Raman spectrum. Transient Raman spectrum has two strong bands at 381 cm^{-1} and 1935 cm^{-1} which are regarded as those of solvated $\text{Cr}(\text{CO})_6$. The vibrational energy relaxation time was measured to be 80-100 ps from both Stokes and anti-Stokes scattering of the 381 cm^{-1} mode. Photodissociation leading to the loss of CO was found to occur within our pulse width of $\leq 5\text{ ps}$ from the depletion of the 533 cm^{-1} mode of ground state $\text{Cr}(\text{CO})_6$. No direct evidence was found for the dynamics of solvent coordination and electronic relaxation on a time scale of $\geq 5\text{ ps}$.

References

1. Lees, A. L. *Chem. Rev.* **1987**, *87*, 711.
2. Simon, J. D.; Xie, X. *J. Phys. Chem.* **1986**, *90*, 6751.
3. Simon, J. D.; Xie, X. *J. Phys. Chem.* **1989**, *93*, 291.
4. Joly, A. G.; Nelson, K. A. *J. Phys. Chem.* **1989**, *93*, 2876.
5. Wang, L.; Zhu, X.; Spears, K. G. *J. Am. Chem. Soc.* **1988**, *110*, 8695.
6. Wang, L.; Zhu, X.; Spears, K. G. *J. Phys. Chem.* **1989**, *93*, 2.
7. Lee, M.; Harris, C. B. *J. Am. Chem. Soc.* **1989**, *111*, 8963.
8. Lee, M.; Harris, C. B. Private Communication.
9. Yu, S.-C.; Xu, X.; Lingle, R. Jr.; Hopkins, J. B. *J. Am. Chem. Soc.* **1990**, *112*, 3668.
10. Chang, Y. J.; Xu, X.; Yabe, T.; Yu, S.-C.; Anderson, D. R.; Orman, L. K.; Hopkins, J. B. *J. Phys. Chem.* **1990**, *94*, 720.
11. Xu, X.; Yabe, T.; Yu, S.-C.; Anderson, D. R.; Orman, L. K.; Hopkins, J. B. *J. Phys. Chem.* **1990**, *94*, 729.
12. Kettle, S. F. A.; Luknar, N. *J. Chem. Phys.* **1978**, *68*, 2264.
13. Welch, J. A.; Peters, K. S.; Vaida, V. *J. Phys. Chem.* **1982**, *86*, 1941.
14. Church, S. P.; Grevels, F. W.; Hermann, H.; Schaffner, K. *Inorg. Chem.* **1985**, *24*, 418.
15. Xu, X.; Lingle, R. Jr.; Yu, S.-C.; Chang, Y. J.; Hopkins, J. B. *J. Chem. Phys.* **1990**, *92*, 2106.
16. Lingle, R. Jr.; Xu, X.; Zhu, H.; Yu, S.-C.; Hopkins, J. B. *J. Am. Chem. Soc.* **1991**, *113*, 3992.
17. Felker, P. M.; Zewail, A. H. *J. Chem. Phys.* **1985**, *82*, 2975.
18. Hopkins, J. B.; Powers, D. E.; Smalley, R. E. *J. Chem. Phys.* **1980**, *72*, 5039.